PAPER

Multi-approach assessment of the spatial distribution of the specific yield: application to the Crau plain aquifer, France

Pierre Seraphin[1] · Julio Gonçalvès[1] · Christine Vallet-Coulomb[1] · Cédric Champollion[2]

Abstract
Spatially distributed values of the specific yield, a fundamental parameter for transient groundwater mass balance calculations, were obtained by means of three independent methods for the Crau plain, France. In contrast to its traditional use to assess recharge based on a given specific yield, the water-table fluctuation (WTF) method, applied using major recharging events, gave a first set of reference values. Then, large infiltration processes recorded by monitored boreholes and caused by major precipitation events were interpreted in terms of specific yield by means of a one-dimensional vertical numerical model solving Richards' equations within the unsaturated zone. Finally, two gravity field campaigns, at low and high piezometric levels, were carried out to assess the groundwater mass variation and thus alternative specific yield values. The range obtained by the WTF method for this aquifer made of alluvial detrital material was 2.9– 26%, in line with the scarce data available so far. The average spatial value of specific yield by the WTF method (9.1%) is consistent with the aquifer scale value from the hydro-gravimetric approach. In this investigation, an estimate of the hitherto unknown spatial distribution of the specific yield over the Crau plain was obtained using the most reliable method (the WTF method). A groundwater mass balance calculation over the domain using this distribution yielded similar results to an independent quantification based on a stable isotope-mixing model. This agreement reinforces the relevance of such estimates, which can be used to build a more accurate transient hydrogeological model.

Keywords Specific yield spatial distribution · Water table fluctuation method · Numerical modeling · Geophysical methods · France

Introduction

For unconfined aquifers, the specific yield S_y, which corresponds to the volume of water released by gravity per unit surface of aquifer and per unit hydraulic head variation (De Marsily 1986), is fundamental for groundwater-mass-balance assessments. Moreover, specific yield data, and their corresponding spatial distribution, are a prerequisite for any transient-groundwater-flow simulation. Specific yield is thus a key parameter, which is generally estimated using pumping or artificial tracer tests. These two in situ methods are

nevertheless highly time-consuming and costly, especially when used to characterize the spatial distribution of an aquifer. At the aquifer scale, transient hydrogeological models of unconfined aquifers require the calibration of a specific yield distribution to simulate accurate water-table fluctuations. These calibrated spatial distributions often produce some unrealistic local values, which are in practice compensated by other poorly constrained parameters or variables such as permeability or recharge rates.

The presented study tested the applicability of alternative methods that can be implemented at a more extensive scale for a spatial characterization of the specific yield. The water-table fluctuation (WTF) method is a widely used and robust analytical method usually applied for estimating groundwater recharge (Moon et al. 2004; Crosbie et al. 2005; Park and Parker 2008; Cuthbert 2010; Jie et al. 2011; Dean et al. 2015). From a theoretical standpoint, this method can alternatively be used to estimate specific yield, if the recharge flux is known; therefore, based on a local water balance, the WTF approach can produce a straightforward estimate of the local

✉ Pierre Seraphin
seraphinpierre@gmail.com

1   Aix Marseille Université, CNRS, IRD, CDF, CEREGE UM 34,
     13545 Aix en Provence, France

2   Géosciences Montpellier, CNRS, UMR 5243, Place E. Bataillon,
     34095 Montpellier Cedex 5, France

specific yield value. Maréchal et al. (2006) already performed such estimation at a seasonal and regional scale. The novelty of this approach is to estimate a spatial distribution of the specific yield by solving the local water balance for multiple major infiltration events recorded at different piezometers. In addition, specific yield is a parameter required when describing water infiltration in the unsaturated zone. Solutions to Richards' equations (RE) by means of models based on the equivalent homogeneous media concept (Miller and Miller 1956) were developed to deal with highly spatially variable aquifer properties, inter alia, the specific yield. Comprehensively reviewed by Vereecken et al. (2007), these approaches propose a unique scaled resolution of RE to reproduce fluid flow in the unsaturated zone and can be used to obtain hydraulic properties by inverse approaches. Very popular in hydrogeology, these methods are directly implemented in numerical codes like Hydrus-1D (Vogel et al. 1996; Simunek et al. 1998); however, to the authors' knowledge, the interpretation of extreme rainfall events by means of a one-dimensional (1D) numerical resolution of RE to assess hydrodynamic parameters was rarely conducted. Finally, some geophysical approaches such as hydro-gravimetry, identify local water storage changes (WSC) estimated from time-lapse gravity data that, in turn, enable the aquifer specific yield to be estimated (Montgomery 1971; Pool and Eychaner 1995; Howle et al. 2003; Hector et al. 2013). The estimates resulting from such an approach are usually only compared to those obtained by in situ methods (pumping and tracer tests).

This study applied each of the approaches previously outlined (WTF method; 1D numerical model solving RE; Hydro-gravimetry) to estimate the poorly known specific yield, enabling transient groundwater modeling of the Crau aquifer. To the authors' knowledge, the use of extreme rainfall events introduced in the first two approaches (WTF and infiltration model) is not very widespread for parameter characterization. These extreme events enable the alternative implementation of the WTF method proposed here, consisting of estimation of the specific yield by knowing the recharge, which is the exact counterpart of the classical WTF approach. Therefore, in the current context of climate change, the predicted increasing occurrence of extreme rainfall events offers the opportunity to implement the methodologies proposed here for media with high infiltration capacity, especially for greatly exploited alluvial-type aquifers.

Hydrogeological setting

The Crau plain aquifer

Located near the Rhône delta, in southern France, the Crau plain (540 km^2 area) is subject to a Mediterranean climate. It is limited on the north side by the Alpilles Range, to the east by the Miramas Hills and on the west by the present-day Rhône River delta (an area also known as "Camargue", Fig. 1). The Crau aquifer is a Quaternary formation created by the accumulation of rough alluvial deposits carried from the Alps by the Durance River. Three paleo-channels of this river were identified in the Crau plain, corresponding to the succession of sea level drops during glacial periods (Colomb and Roux 1978). Three main sedimentation episodes (2 Ma, 200 ka, and 20 ka) have produced a primary porosity, formed by coarse elements (pebbles), filled by sandy clays, thus constituting the main phreatic aquifer of the region. This detrital material of alluvial origin presents an average thickness of 13 m, mostly unconsolidated, but can be locally cemented, forming a puddingstone.

At present, there is no natural river network over the Crau plain and all the surface-water transfers occur through an artificial irrigation network of canals. The absence of a river network is due to the very flat topography combined with the high infiltration capacity of ground surfaces, where the detrital formation outcrops with almost no soil cover. Nevertheless, a large proportion of the Crau plain is covered by artificial grasslands (140 km^2 in 2014), where well-developed soil layers result from a long-term traditional flood irrigation practice (Courault et al. 2010).

Starting nearly 500 years ago, the cultivation of grasslands for hay production is still the main agricultural activity of the Crau plain. Highly water-consuming, the irrigation practice provides water to meadows from mid-March to late October and produces high return flows (Mailhol and Merot 2007; Courault et al. 2010). Indeed, previous studies showed that the recharge of the Crau aquifer is mainly caused by irrigation excess (Olioso et al. 2013). This anthropogenic control produces large seasonal water-table fluctuations reaching up to 8 m recorded in the most irrigation-influenced piezometers.

Only a few specific yield data are available (see Table 1). Whether calculated using geochemical tracer methods or transient pumping tests, these scarce data are mainly located on the most productive paleo-channel (to the east of the aquifer), where pumping well performance studies were conducted. However, some spatial distributions of the specific yield have also been proposed by calibrating transient hydrogeological models (Bonnet et al. 1972; Berard et al. 1995). According to Bonnet et al. (1972), their approach did not provide accurate estimates due to a lack of permeability measurements and the unfulfilled assumption of no recharge during the application periods. The model by Berard et al. (1995) produced, after trial and error modifications, specific yields ranging from 1 to 18%; however, the physical relevance of this spatial distribution obtained by calibrating both permeability and recharge can be questioned for equifinality reasons (Beven 1993). Although challenging, it is thus desirable to produce a new spatial distribution of the specific yield using, as far as possible, methods independent from any hydrogeological model calibration.
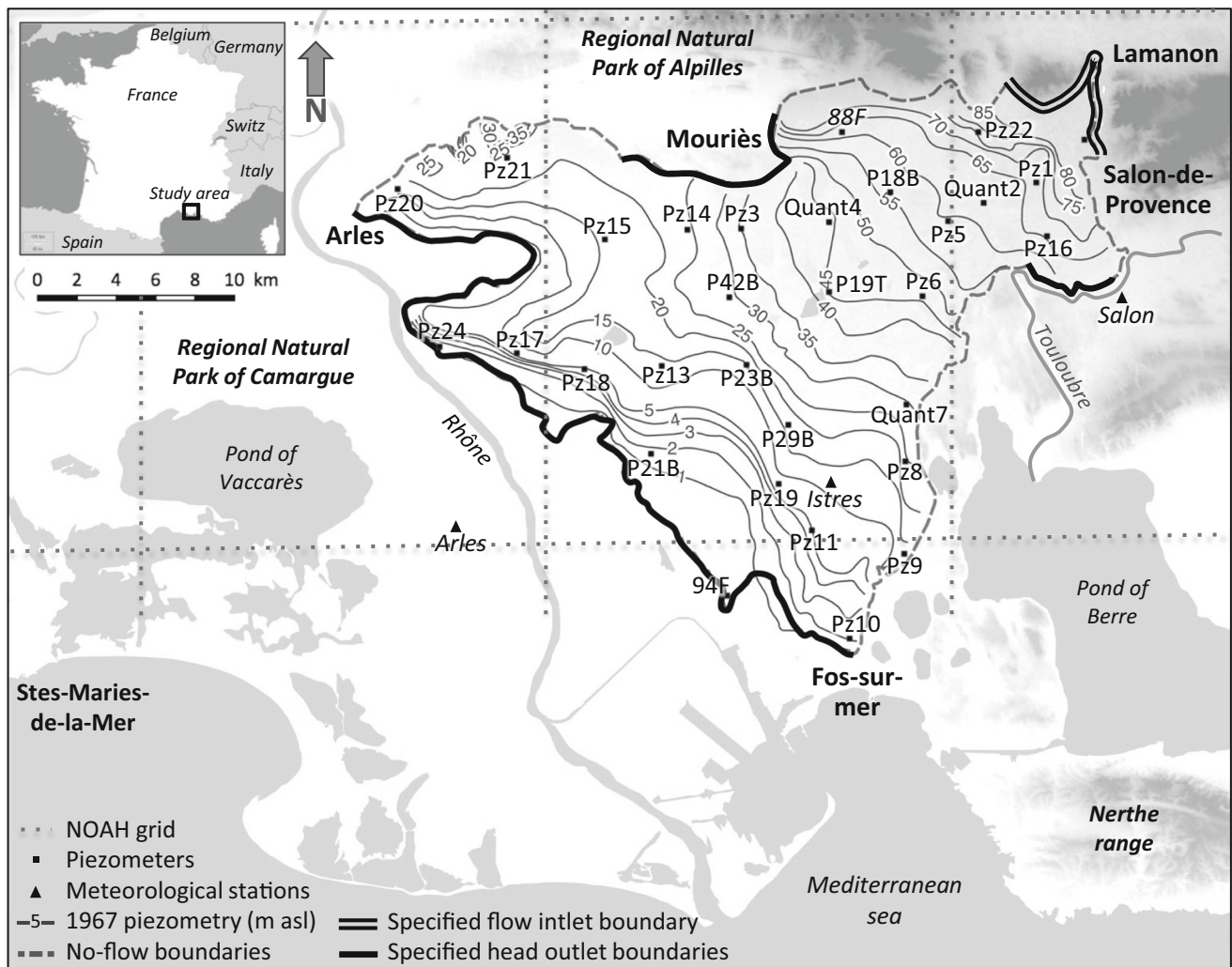
Fig. 1 Hydrogeological context of the Crau aquifer, showing boundary conditions and the 1967 piezometric contour map extracted from Albinet et al. (1969). Shades of gray represent the reliefs

Hydrological data

The hydrological time series used in this study are accessible from public French governmental databases. Rainfall data at three stations (Fig. 1) were extracted from the French meteorological database (Météo-France 2016): Salon-de-Provence station (ID: 13103001) on the east side of the Crau plain; Istres station (ID: 13047001) in the middle; and Arles "Tour du Valat" station (ID: 13004003) on the west side.

Water-table elevation data were extracted from the groundwater database "ADES" (BRGM 2016a). Two piezometer networks with daily records are available over the Crau

Table 1 Specific yield data obtained by in situ methods

ID	X (WGS84)	Y (WGS84)	S_y	Method	Reference
09938X0127/P1	4.95878	43.64889	0.06	Pumping test	Garnier and Syssau (1976)
09938X0077/F	4.95198	43.57604	0.065		Forkasiewicz (1972)
09945X0236	5.03757	43.63758	0.085		ANTEA (1995)
Coussoul Merle	5.00187	43.65213	0.11		J. Gonçalvès (2014, unpublished data)
Pz21/25 SPSE	4.88370	43.52560	0.125	Average between tracer test (0.15) and model (0.1)	Boissard (2009) Maier (2010)
P1/P2/P3/P4 SNCF	4.96627	43.58332	0.164	Average of multiple tracer tests (0.111 to 0.217)	Jourde and Brunet (2001)

aquifer (Table 4): the French Geological Survey (BRGM) network with eight piezometers dating back to 2002–2003, and the Crau Plain Groundwater Union (SYMCRAU) network with 23 recently drilled piezometers (hydraulic head records starting in 2012–2013). One of the three meteorological stations was assigned to each piezometer (Table 2) according to the Thiessen polygons spatialization method (Fiedler 2003).

Materials and methods

Three methods were used to obtain relevant specific yield data. The first two use the abrupt water-table responses to major rainfall events, either through a global water balance approach based on the water-table fluctuation (WTF) method, or with 1D vertical transient flux modeling. They take advantage of the Mediterranean climate of the study area, characterized by heavy and isolated rainfall episodes, and of the high infiltration capacity of the Crau aquifer, which lead to a short response time of the water table to rainfall. The third method is based on the interpretation of two gravity surveys performed for this study.

Identification of the major rainfall events

Rainfall events recorded by three meteorological stations (Fig. 1) were carefully selected outside the irrigation seasons (late October until early March) to prevent any bias related to locally constrained recharge by irrigation. The selection criterion used here is a precipitation amount greater than 50 mm causing a groundwater-level rise greater than 0.5 m, in order to ensure a prominent infiltration process as compared to possible storage variations in the unsaturated zone (values selected to obtain, at least, two clear events per piezometer). Given the high infiltration capacity of the soil (Bader et al. 2010; Courault et al. 2010) and of the alluvial materials, a weak runoff can be assumed over the Crau plain, even during extreme rainfall events (Dellery et al. 1964). Indeed, acknowledging the amount of precipitation and maximum intensities (Table 2), and providing a maximum value of 2 mm d^{-1} for the mean winter potential evapotranspiration (PET) over the 1991–2011 period (a value that can be even lower during cold weather periods; Météo-France 2016), these winter rainfall events can thus be considered as entirely recharging the aquifer. The availability of an hourly time step piezometric record is an additional criterion for the application of the 1D infiltration modeling. Showing various precipitated amounts, durations, and preceding rainfall conditions, the selected events presented in Table 2 constitute a good representation of the diversity of the major rainfall events occurring over the region.

Water-table fluctuation method

The WTF method, which is one of the most widespread approaches for estimating groundwater recharge (Sophocleous

1991; Hall and Risser 1993; Crosbie et al. 2005; Cuthbert 2010), was thoroughly reviewed by Healy and Cook (2002). Based on a local groundwater balance equation, an observed rise in the piezometric level is interpreted in terms of surface groundwater recharge. During a given time period Δt (s) of recharge R (m s^{-1}), the water-table variation ΔH (m), multiplied by the specific yield S_y, reflects the local water mass balance; i.e. precipitation P (m s^{-1}) *minus* runoff r (m s^{-1}), evapotranspiration from the water table E (m s^{-1}), and the net groundwater drainage rate D (m s^{-1}) that can be natural or affected by water uptakes. This water balance is written:

$$\left(\frac{\Delta H}{\Delta t}\right)_R S_y = P - (r + E + D) \tag{1}$$

In addition, the Lisse effect can also cause an abrupt water level increase by trapping air between the wetting front and the water table (Heliotis and DeWitt 1987) in the case of intense infiltration events. This process amplifies the water level rise, especially in the case of a very shallow water table with an unsaturated zone thickness of less than 1 m (Weeks 2002). Since, according to the digital elevation model (GO-13 2009) and the 2013 piezometric map (Seraphin et al. 2016), the average unsaturated zone thickness of the Crau aquifer is greater than 6 m, this process can be neglected; moreover, all the piezometers used in this study present unsaturated zone thicknesses greater than 1 m.

In order to apply this method for assessing specific yield values based on a known recharge value, some simplifications were made. As detailed in section 'Identification of the major rainfall events', the high infiltration capacity of the soil and the alluvial materials (locally outcropping) mean that the entire rainfall can be assumed to infiltrate (i.e. $r \approx 0$), and the application of the method to only winter rainfall events makes the evapotranspiration negligible compared to the rainfall volumes (i.e. $E \approx 0$). The use of Eq. (1) to determine S_y requires the net groundwater drainage rate D to be ascertained for a given piezometer. D was estimated graphically using a linear regression (see Fig. 2 for a schematic plot of the methodology) when no recharge R can be assumed, i.e. during dry periods when $P = R = 0$ in Eq. (1) giving:

$$D = \left(\frac{\Delta H}{\Delta t}\right)_{R=0} S_y \tag{2}$$

Then, introducing Eq. (2) into Eq. (1) for a given major rainfall event ($R > 0$) with $r = E = 0$ yields:

$$S_y = \frac{P}{\left(\frac{\Delta H}{\Delta t}\right)_R + \left(\frac{\Delta H}{\Delta t}\right)_{R=0}} \tag{3}$$

where $\left(\frac{P}{\Delta t}\right)_R$ represents the ratio of P over $(\Delta t)_R$, with $(\Delta t)_R$ the

Table 2 Description of the major rainfall events recorded in the three meteorological stations

Date of the event (dd/mm/yyyy)	Arles station				Istres station				Salon station			
	P (mm)	Length (h or d)	Max intensity (mm h^{-1} or mm d^{-1})	No. of previous days with $P < 2$ mm	P (mm)	Length (h or d)	Max intensity (mm h^{-1} or mm d^{-1})	No. of previous days with $P < 2$ mm	P (mm)	Length (h or d)	Max intensity (mm h^{-1} or mm d^{-1})	No. of previous days with $P < 2$ mm
Hourly resolution (mm h^{-1})												
30/11/2003	–	–	–	–	120.2	99	14.4	4	98.4	98	12.6	4
22/10/2009	–	–	–	–	86.8	12	21.8	11	80	13	20	11
25/11/2014	–	–	–	–	129.2	279	6.5	9	113.3	272	12.5	9
Daily resolution (mm d^{-1})												
01/12/2003	173.1	9	121.7	1	120.2	9	86	1	104.8	9	76.2	1
27/01/2006	40.8	12	26.8	10	37.8	12	28.8	10	45.2	12	40	10
22/11/2007	69.8	9	62.2	24	67	9	59.6	25	86.2	9	73	25
04/01/2008	69.6	19	19.4	11	77.4	19	24.6	24	68.8	19	25.2	24
02/11/2008	92.4	30	58.7	1	111	30	58.6	1	96.2	30	41.4	1
09/12/2008	74.1	15	37.9	9	103.2	15	53.4	9	100	15	46	9
25/01/2009	58.8	6	24.8	14	56.2	6	22.8	14	35.4	6	10.2	14
01/02/2009	102.3	7	47.5	4	45.8	7	18.8	4	35.4	7	9.8	4
21/10/2009	79.9	5	59.4	11	124.6	5	87	11	146.8	5	80	11
29/11/2009	43.5	9	23	27	63.8	9	38.4	26	118.3	9	78.5	27
21/12/2009	53.8	6	26.9	8	65	6	33.6	17	84	6	39.8	17
07/01/2010	64.4	3	40	4	61.6	3	38.6	4	43.2	3	26.8	2
18/12/2013	45.6	3	29	29	52.6	3	30.9	29	67.4	3	47.9	27
18/01/2014	60.5	2	33.2	4	42.9	2	22	4	47.6	2	25.6	1
29/01/2014	37.1	4	24.2	9	79.8	4	36.7	8	84.5	4	43.4	8
03/02/2014	55.2	8	25	1	55.7	8	24.5	1	81.2	8	30.9	1
10/10/2014	12.6	1	12.6	10	38.4	1	38.4	9	74.2	1	74.2	9
09/11/2014	71.7	7	26.1	3	76.5	9	43.9	3	125.6	9	79	4
24/11/2014	150.7	13	41.2	9	129.2	13	37.9	9	113.3	13	64.1	9
18/01/2015	44.2	4	21	1	70.8	4	32	1	52	4	19.8	1

time period corresponding to the piezometric rise (see Fig. 2).

The associated uncertainty (ignoring the errors from all other assumptions, i.e. $r = E = 0$) is given by the linear regression used to identify D:

$$\sigma_{Sy}{}^2 = \left(\frac{\partial S_y}{\partial \left(\frac{\Delta H}{\Delta t}\right)_{R=0}}\right)^2 \sigma_{\left(\frac{\Delta H}{\Delta t}\right)_{R=0}}{}^2 \tag{4}$$

To summarize, the three steps of the WTF method implemented on daily time series are:

– Selection of a large rainfall event P (Table 2) producing a continuous piezometric rise greater than 0.5 m during a period of recharge Δt.
– Identification of $\left(\frac{\Delta H}{\Delta t}\right)_{R=0}$ by linear regression on piezometric-level time records during a dry period (Fig. 2). This term is estimated in a similar temporal and water-level elevation window to that of the piezometric rise $\left(\frac{\Delta H}{\Delta t}\right)_R$ (Fig. 2) since Crosbie et al. (2005) and Cuthbert (2014) already showed that there is a correlation between water-table elevations (H) and net groundwater drainage rate (D), especially when the water-table fluctuations are great enough to significantly modify the local transmissivity (see section 'Method validation' for details). Hence, this step yields a value representative of the average net groundwater drainage rate occurring during the studied piezometric rise.
– Solving Eq. (3) where $\left(\frac{\Delta H}{\Delta t}\right)_R$ is identified according to the graphical method shown in Fig. 2.

Hence, applied to many winter rainfall events, the WTF method can be used to estimate the specific yield, and its associated standard deviation, in the vicinity of piezometers presenting daily precipitation and piezometric records.

Estimating infiltration across the unsaturated zone

Here it is proposed to infer some unconfined aquifer properties, inter alia, the specific yield, using an approach consisting of simulating the flow of water across the unsaturated zone during a well-defined infiltration event, recorded at an hourly time step (Table 2). For this purpose, the piezometric response to a major rainfall event recorded at an hourly time step was used, of which the purely 1D vertical infiltration signal has to be isolated from the piezometric level record by a graphical detrending. Once identified, this measured purely infiltration signal is interpreted using a 1D vertical numerical model solving RE to obtain, by an inverse approach, the hydraulic parameters and especially S_y.

Theoretical background

Considering a 1D vertical motion of water mostly under the effect of gravity across a soil, the 1D transient mass balance equation in the unsaturated zone is written:

$$\frac{\partial}{\partial z}\left[\rho \frac{K(\theta)}{\mu}\left(\frac{\partial P}{\partial z} + \rho g\right)\right] = \frac{\partial(\rho\theta)}{\partial t} \tag{5}$$

where θ ($m^3\ m^{-3}$) is the soil moisture content, P (Pa) the pore pressure, ρ ($kg\ m^{-3}$) the water density, μ ($kg^{-1}\ s^{-1}$) the coefficient of dynamic viscosity, g ($m\ s^{-2}$) the acceleration due to gravity, $K(\theta)$ ($m\ s^{-1}$) the unsaturated hydraulic conductivity, z (m) the vertical axis, and t (s) the time.

Assuming constant ρ and μ, and introducing $h = -\frac{P}{\rho g}$ (m), the unsaturated-zone water matric potential (i.e. absolute value of the soil-water pressure head), Eq. (5) writes as:

$$\frac{\partial}{\partial z}\left(-K(\theta)\frac{\partial h}{\partial z} + K(\theta)\right) = \frac{\partial \theta}{\partial t} = \frac{\partial \theta}{\partial h}\frac{\partial h}{\partial t} \tag{6}$$

This non-linear partial differential equation can only be solved numerically upon the introduction of constitutive relationships relating the hydraulic conductivity and the pore pressure to the soil moisture. Similar to Warrick and Hussen (1993), the Brooks-Corey model (Brooks and Corey 1964) was used here:

$$\left(\frac{\theta - \theta_r}{\theta_s - \theta_r}\right) = \left(\frac{h_e}{h}\right)^\lambda \text{ with } h < h_e < 0 \text{ leading to } \frac{\partial \theta}{\partial h}$$
$$= -\lambda(\theta_s - \theta_r)\frac{h_e^\lambda}{h^{\lambda+1}} \tag{7}$$

with λ (−) the pore-size distribution index, h_e (m) the air entry potential, θ_r ($m^3\ m^{-3}$) the residual water content, and θ_s ($m^3\ m^{-3}$) the saturated water content.

The Brooks-Corey relationship between unsaturated $K(\theta)$ and saturated conductivities K_s is:

$$K(\theta) = K_s\left(\frac{\theta - \theta_r}{\theta_s - \theta_r}\right)^{\frac{2+3\lambda}{\lambda}} \tag{8}$$

Introducing Eq. (7) into Eq. (6), noting that $S_y = \theta_s - \theta_r$, the RE is written as:

$$\frac{\partial}{\partial z}\left(K(\theta)\frac{\partial h}{\partial z} - K(\theta)\right) = \lambda S_y \frac{h_e^\lambda}{h^{\lambda+1}}\frac{\partial h}{\partial t} \tag{9}$$

The numerical resolution of Eq. (9) reproduces a wetting front propagation into the soil and thus the associated water-table rise. Therefore, reproducing infiltration data (e.g. water-table rise) using a numerical solution of Eq. (9) requires calibrating four parameters: K_s, S_y, λ, h_e; however, this number reduces to three by considering a clear linear relationship

Fig. 2 Example of WTF interpretation after the November 2014 rainfall event at piezometer P42B. The dashed line represents the linear regression used to compute the net groundwater drainage (D)
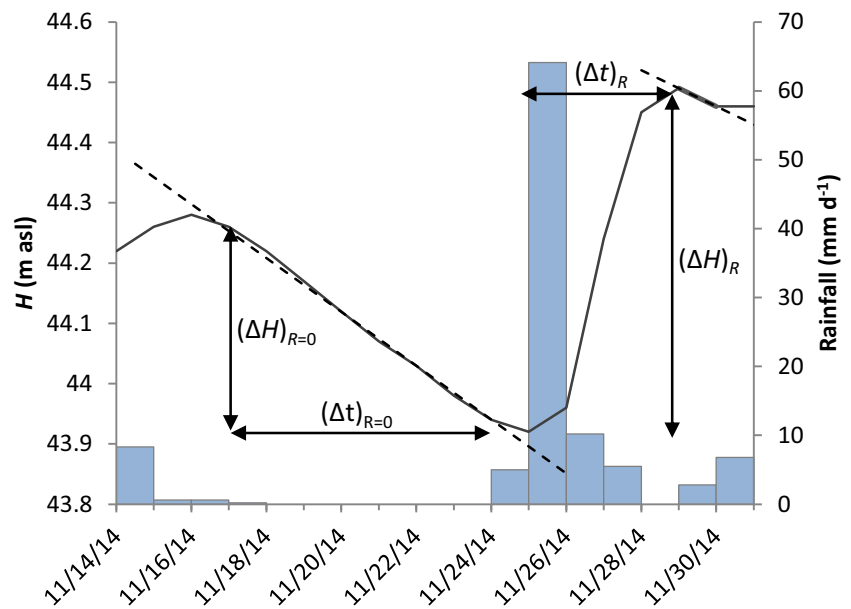
between λ and h_e shown by the data of Rawls et al. (1982) for various soil types.

Numerical analysis and implementation of the infiltration model

In order to simulate the wetting front propagation during a major rainfall event, REs are solved using a finite differences scheme with an iterative algorithm to treat the non-linearity of both the spatial and temporal terms of the pressure diffusion Eq. (9). A regular grid with 10-cm spacing is used and a time step of 10 s is also required to obtain convergence. The boundary conditions are no flow at the bottom (substratum of the aquifer) and the precipitation rate at the top of the soil column. As mentioned in section 'Identification of the major rainfall events', the high infiltration capacity of the Crau aquifer (Dellery et al. 1964), and the use of only extreme rainfall events (Table 2) occurring during winter (i.e. insignificant evapotranspiration), mean that the entire rainfall volume can be assumed to reach the water table, producing a significant piezometric rise (> 0.5 m). The initial condition used in the simulations is a soil moisture profile at hydrostatic equilibrium with the water table. This is a realistic condition because model calculations predict that several days (1 week maximum) are required to recover a hydrostatic profile after a rainfall event, and the considered events show at least 4 days without significant rainfall (upper part of Table 2). The model is calibrated by matching the simulated and measured time-varying water-table elevation due only to the assumed 1D infiltration process. The required purely infiltration observed signal is isolated from the piezometric level record by detrending the piezometric signal to remove the net groundwater drainage contribution

(assumed to be linear for a short time period, see Fig. 3). In the inversion process, the a priori range of hydraulic conductivity K_s, pore-size distribution index λ, and specific yield S_y are considered to model the piezometric rises using hourly precipitation data as input. The basic inversion used here consists of a uniform sampling (regular spacing) in the parameter space (K_s, λ, S_y; note that h_e is given by a linear relationship with λ) and subsequent repeated direct simulations of the infiltration event. Therefore, by looping this RE resolution, the model enables a set of variables to be selected that produces the best agreement between simulated and observed piezometric level increase due to infiltration. Python 2.7 (Oliphant 2007; Millman and Aivazis 2011) was used to implement and solve this numerical scheme. Such treatment of the RE has already been validated in two-dimensional (2D) by an experimental base case where all the parameters were known and imposed (Rivière et al. 2014).

Gravimetry

Water storage changes (WSC) lead to variations in the Earth's gravity field that can be measured. Hydrogravimetry is increasingly used and can be applied at regional scale, using satellite gravity measurements (Becker et al. 2011; Gonçalvès et al. 2013; Ramillien et al. 2014), or at a more local scale, using ground-based gravimeters (Hector et al. 2013). While absolute gravimeters (10–20 nm s^{-2} accuracy) directly measure the acceleration of a mass during free fall in a vacuum, more compact spring-based relative gravimeters (accuracy around 50 nm s^{-2}, depending on the field conditions; Bonvalot et al. 2008; Merlet et al. 2008; Jacob et al. 2010) give access to spatial gravity variations with respect to a base station, and can

thus provide spatial and temporal variations with repeated measurements. For further details on the different gravimeters and methods, see for instance the review by Melchior (2008). Local WSC estimated from time-lapse gravity data have many hydrological applications such as constraining hydrogeological models (Jacob 2009; Naujoks et al. 2010; Christiansen et al. 2011), identifying water transfers (Kroner and Jahr 2006; Chapman et al. 2008; Jacob et al. 2008), but also providing estimates of aquifer specific yield (Montgomery 1971; Pool and Eychaner 1995; Howle et al. 2003; Hector et al. 2013). Hence, this section presents the method followed to infer specific yield from gravity measurements performed with the spring-based relative gravimeter Scintrex Autograv CG-5 #167 provided by the Institut National des Sciences de l'Univers (INSU).

Survey setup and data processing

The gravity network consists of two loops that begin and end at a reference station (Pz10; Fig. 1) in order to correct drift. Two piezometric and gravity surveys were performed on 24 piezometers (represented by black squares on Fig. 1): one from September 22 to 25, 2014, at the end of the irrigation season, and the other one from March 1 to 4, 2015, just before the beginning of the irrigation period. For the two surveys, the same relative gravimeter was used (CG5 #167) with a resolution of 10 nm s^{-2} and a repeatability less than 100 nm s^{-2} (Scintrex Ltd. 2006). Dates were selected according to the hydrological cycle mainly controlled by irrigation practice in order to observe the larger piezometric fluctuations, and thus produce accurate estimates of the specific yield. Unfortunately, rainfall events occurred during the two surveys, creating significant WSC in the unsaturated zone and reducing the piezometric variation of some measurement points. The piezometer presenting the lowest water-table fluctuations and the smallest unsaturated zone thickness (Pz10) was used as a reference station and measured three times a day in order to correct gravimetric drifts.

Relative gravity measurements are subject to drifts and external processes (e.g. earth and ocean tides, air pressure changes), which were corrected using a standard approach (Deville 2013). Lederer (2009) proposes a good review of the magnitude of these errors, including a characterization of the Scintrex Autograv CG-5 precision. Estimation of the gravity network including the drift was performed following a least square approach using the software package MCGRAVI (Beilin 2006) based on the inversion scheme of GRAVNET (Hwang et al. 2002). The accuracy of the gravity measurements is difficult to estimate, but based on the residuals of the network adjustment, the mean residual is around 15 nm s^{-2} (10 for the first and 20 nm s^{-2} for the second survey).

Inferring porosity from gravimetry measurements

A first-order direct estimate of the gravitational effect of WSC can be achieved by applying the Bouguer plate model:

$$\Delta g = 2\pi\rho G \, \Delta w \tag{10}$$

where ρ is the density of water (kg m^{-3}), G is the universal gravitational constant (m^3 kg^{-1} s^{-2}), Δg is a variation of gravity measurements (m s^{-2}), and Δw is the corresponding variation of thickness of an infinite water layer (m), i.e., the WSC.

Regarding an alluvial aquifer, this WSC Δw corresponds to water storage change in the unsaturated zone ΔS (m) plus the variation in groundwater storage, which corresponds to the variation in the water-table elevation ΔH (m) times the specific yield S_y for an unconfined aquifer.

Hence, using Eq. (10), the specific yield and its associated error can be expressed by:

$$S_y = \left(\frac{\Delta g}{2\pi\rho G} - \Delta S\right) \frac{1}{\Delta H} \tag{11}$$

$$\sigma_{S_y}^2 = \sigma_{\Delta g}^2 \left(\frac{\partial S_y}{\partial \Delta g}\right)^2 + \sigma_{\Delta H}^2 \left(\frac{\partial S_y}{\partial \Delta H}\right)^2 \tag{12}$$

Results

Water-table fluctuation method results

Method validation

In order to validate the method and to estimate the impact of the spatial heterogeneity of the precipitations, the alternative WTF method presented in this study was first applied using long-term time series at two specific piezometers (P42B and P29B) located in different hydrological conditions. P42B is located close to irrigated meadows and presents rapid piezometric responses to infiltration events (weekly variations) mostly controlled by irrigation return flow. Conversely, P29B, located far from any meadow, shows a piezometric signal characteristic of a purely natural recharge with monthly infiltration durations. The mean and standard deviation of the specific yields obtained by alternative use of the rainfall events recorded by each of the three available meteorological stations are presented in Table 3. The records of the three stations were used for this validation step to estimate the influence of the spatial and temporal heterogeneity of the rainfall on the results (see section 'Water-table fluctuation method: discussion').

These repeated applications of the WTF method also provide a set of estimates for the net groundwater drainage

Fig. 3 The 22nd of October 2009 rainfall event observed at piezometer P42B. The dashed line represents the linear regression used to detrend and thus to remove the net groundwater drainage contribution from the piezometric signal

$y = -0.0007x + 28.734$
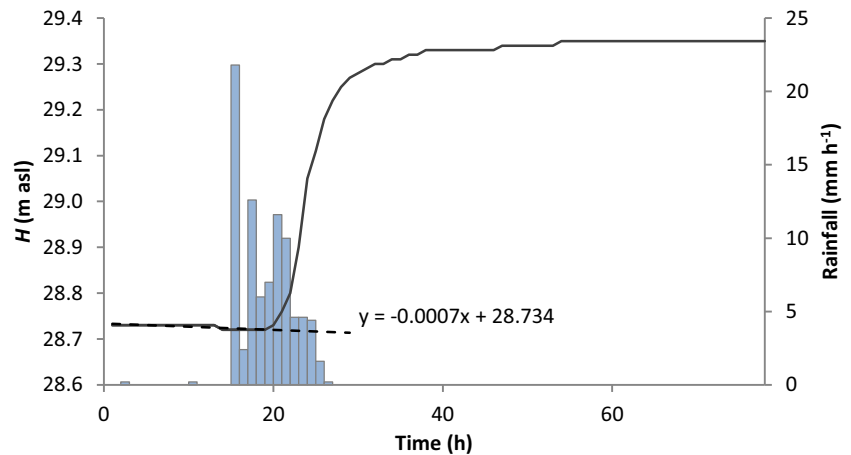
rate. Assumed constant for an ideal aquifer (Cuthbert 2014), Fig. 4a,b shows hydraulic head-dependencies of the computed net groundwater drainage rates (D; using Eq. 2) for piezometers P42B and P29B. These clear linear relationships are explained by: (1) large water-table fluctuations compared to the aquifer thickness, implying significant transmissivity variations over time; (2) a heterogeneous recharge process redistributing water within both the unsaturated and saturated zones due to a strong heterogeneity of the aquifer materials (Cuthbert 2014). Also observed by Crosbie et al. (2005), these linear relationships illustrate the consistency of the net groundwater drainage estimates derived as part of this study.

This hydraulic head-dependency of the net groundwater drainage offers a valuable opportunity to assess the mean local recharge since these linear regressions make it possible to convert an average water level, representative of an interannual steady state, into a net groundwater drainage rate (using equations in Fig. 4a,b), which thus corresponds to the average value of the local recharge. Using the long-term mean water level of P42B (28.89 m asl over 12 years), a 1,339-mm year^{-1} value was obtained for the average recharge in the vicinity of this piezometer, influenced both by irrigation return flow and precipitation. Subjected only to natural recharge, P29B yields 116 mm year^{-1} of mean recharge using an average value of 16.38 m asl for the water level (over 12 years). The subtraction yields 1,223 mm year^{-1} of recharge by irrigation return flow and 116 mm year^{-1} of natural recharge, which is consistent with the values obtained by previous studies using geochemical tracers at the aquifer scale (Seraphin et al. 2016; i.e. 1,109 ± 202 mm year^{-1} of recharge by irrigation return flow, and 128 ± 50 mm year^{-1} of natural recharge), and local scale (Vallet-Coulomb et al. 2017; i.e. 1,190 ± 380 mm year^{-1} of recharge by irrigation return flow, and 160 ± 100 mm year^{-1} of natural recharge). These results represent an independent validation of the application of the WTF method proposed here.

Application to the entire Crau plain

The WTF method was then applied to the rainfall events of winters 2013–2014 and 2014–2015 (Table 2), when the most complete piezometric level data set was available, in order to obtain the best spatial distribution of the specific yield. Only between two to six infiltration events can be interpreted for each piezometer, because of the spatial heterogeneity of some rainfall events and the different magnitudes of the water-table responses of different piezometers to the same precipitation volume (caused by the variability of the specific yield). As previously explained, using only large rainfall events (> 50 mm) producing significant piezometric rises (> 0.5 m) reduces the importance of the long-term unsaturated zone storage in the local water mass balance. The mean values of the specific yield obtained by the WTF method and their related standard deviations (including the error on the net groundwater drainage estimates) are presented in Table 4.

One-dimensional infiltration model results

This approach was applied to infiltration events recorded in six piezometers (see the following), but only one simulation is detailed hereafter. The infiltration process considered here occurred on piezometer P42B after the rainfall event of October 22, 2009 (86.8 mm during 12 h with a maximum intensity of 21.8 mm h^{-1} measured at Istres station) causing a rise of 0.62 m in the water table during the following 36 h (Fig. 3). Assuming that the entire rainfall amount reaches the water table, a rapid application of the WTF method yields a first estimate of the specific yield of about 16%. As stated in section 'Numerical analysis and implementation of the infiltration model', three parameters have to be inferred by uniform sampling of the parameter space and subsequent direct simulations: K_s, S_y, and λ. Regarding permeability (K_s), data measured in some boreholes (Porchet 1930; BRGM 2016b) surrounding piezometer P42B (3 km) showed values between 5.10^{-4} and 1.10^{-2} m s^{-1}. This preliminary work meant that

the tested ranges of permeability (from 1.10^{-4} to 5.10^{-2} m s^{-1} every half order of magnitude) and porosity (from 12 to 20% every 2%) could be reduced, thus increasing the calculation speed. The pore-size distribution index (λ) was systematically tested between 0.2 and 0.5 (every 0.05) according to the measured values of Rawls et al. (1982). To illustrate the approach, the misfit function (root-mean-square error based on hourly simulated and observed data) for piezometer P42B is presented in Fig. 5a and shows a minimum error for a specific yield of 18% among the 210 simulations performed. But after a finer parameter space exploration—K_s tested between 1.10^{-3} and 9.10^{-2} m s^{-1} every 1/5th order of magnitude (1.10^{-3}, 3.10^{-3}, 5.10^{-3}, 7.10^{-3}, 9.10^{-3}, 1.10^{-2},…); S_y tested with 17, 18 and 19%; λ still tested between 0.2 and 0.5 every 0.05—the best simulation among these 150 new simulations (Fig. 5b) was obtained for a permeability of 9.10^{-3} m s^{-1}, a pore-size distribution index of 0.5, and a specific yield of 17% (consistent with the 16% estimated at the beginning of this section by the WTF method).

Hydro-gravimetry results

Average value of S_y at the aquifer scale

Figure 6 represents the results of the hydro-gravimetric survey (March 2015 data *minus* September 2014 data). The plot shows a correlation between gravimetric and piezometric variations (Δg versus ΔH). Shifts of the regression intercept reflect average WSC in the unsaturated zone of the Crau aquifer plus WSC of the reference station (Pz10); hence, the three red dots, far from the linear trend (Pz20, Pz21 and 88F), present different unsaturated zone storage variations from the rest of the aquifer and are not accounted for in the plotted linear regression. This is likely due to the clay beds, observed on stratigraphic logs (BRGM 2016b), above the water-table variations of these zones. Using the 420 nm s^{-2} m^{-1} gradient, derived from the Bouguer plate analytical expression (Eq. 10), it is possible to interpret the slope and the intercept of this linear regression in terms of specific yield and unsaturated zone water storage variation (mean and standard deviation) at the aquifer scale. Thus, not considering the three particular points, the Crau aquifer presents an average specific yield S_y of $12.3 \pm 1.9\%$, and a variation of the unsaturated zone water storage ΔS between September 2014 and March 2015 of 0.121 ± 0.025 m. This average variation of unsaturated zone water storage was calculated considering 0.07 m of water-table fluctuation and no WSC in the unsaturated zone of the reference station (Pz10).

Point-scale measurements

The simplest way to correct the shift of the gravity measurements created by WSC in the unsaturated zone consists of subtracting the intersection of the linear regression (Fig. 6). Doing this simplified average WSC correction, the application of Eq. (11) leads to eight unrealistic specific yield values out of the 24 estimates (Table 2), because of the heterogeneous soil distribution over the Crau plain. Note also that the standard deviations, computed using Eq. (12), are globally too high to characterize the precision of most of the values, especially for piezometers presenting low water-table fluctuations between September 2014 and March 2015.

An alternative attempt was tried to perform a physically based correction of ΔS, using unsaturated zone storage data extracted from the Global Land Data Assimilation System (NASA 2016). The NOAH model (Rodell and Beaudoing 2013) provides monthly soil moisture values (up to 2 m depth) at a $0.25° \times 0.25°$ grid resolution. The resolution and the proximity to the coastal shore only allow three meshes to be extracted covering the north part of the Crau plain (Fig. 1). Each piezometer within a NOAH mesh grid was directly corrected using the respective NOAH soil moisture variation ΔS (no improvements observed using any kind of interpolation of NOAH ΔS estimates), expect for Pz9 and Pz10 (in the absence of NOAH mesh at this precise location; Fig. 1), corrected using the neighboring mesh to the north. The mean NOAH soil moisture variation between September 2014 and March 2015 was about 0.2 m, in good agreement with the mean value discussed in the previous section (i.e. 0.121 ± 0.025 m). The southern and mostly unirrigated part of the Crau plain is not covered by the simulated NOAH soil moistures. However, considering the absence of substantial pedologic layers, the regional variation at this location should be lower than in the northern part of the Crau plain, in better agreement with the value obtained with hydro-gravimetric data. Using these NOAH unsaturated zone storage data to correct gravity measurements of piezometers within each grid cell (corrections represented by gray dots on Fig. 6) provides new estimates of the specific yield (Table 4) showing seven unrealistic values.

Discussion

Table 4 presents the specific yield values obtained by applying alternatively the three different methods. The following sections discuss and compare these approaches.

Water-table fluctuation method

This simple method allows a straightforward estimation of the specific yield using all the piezometers of the Crau aquifer presenting daily piezometric data. The two main sources of uncertainties are (1) the vertical recharge estimate, which depends on the precipitation estimate and on the assumption that the entire precipitated amount reaches the water table without

Table 3 Results of multiple interpretations of large rainfall events by WTF method performed on P42B and P29B using the longest piezometric time-series with different meteorological stations. *SD* standard deviation

Borehole	No. of events	Mean $S_y \pm$ SD per meteorological station			Mean $S_y \pm$ SD for the three stations
		Arles	Istres	Salon-de-Provence	
P42B	11	9.0 ± 4.6%	10.2 ± 4.7%	10.7 ± 6.6%	9.9 ± 0.8%
P29B	8	9.5 ± 3.6%	10.5 ± 3.5%	9.0 ± 4.0%	9.6 ± 0.8%

substantial evapotranspiration, runoff, or unsaturated zone storage variations, and (2) the quantification of the net groundwater drainage rate. The hypothesis of an effective infiltration corresponding to the entire precipitation may produce overestimated specific yield values, especially because of possible water retention in the unsaturated zone. Applying the WTF method on several major rainfall events mitigates the impact of this assumption, however. The results obtained by the WTF method (Table 4) appear to be remarkably consistent with the ranges and locations of the few values reported in the literature (Table 1; Fig. 8).

The specific yield values of P29B and P42B, computed using only the few rainfall events that occurred during the studied period, are 8.3 ± 0.5% (*n* = 2) and 9.2 ± 1.5% (*n* = 3) respectively (Table 4), which is very similar to the value computed using all the events measured at Istres meteorological station (Table 3), i.e. 10.5 ± 3.5% (*n* = 8) and 10.2 ± 4.7% (*n* = 11) respectively. This confirms the reliability of the mean specific yields computed using the few WTF interpretations performed on a period presenting major rainfall events. Table 3 also shows that the heterogeneity of the rainfall distribution, and thus the choice of meteorological station impacts the results, especially for the interpretation of smaller rainfall events. By using various interpretations however (see section 'Method validation'), this uncertainty on rainfall value is much lower than that created by the variations in unsaturated zone storage—standard deviation (SD), by considering the three meteorological stations (e.g. 0.8% for P42B) much lower than the SD created by multiple WTF interpretations per station (e.g. 4.6–6.6% for P42B; see Table 3).

One-dimensional infiltration model

More time- and CPU-consuming than the WTF interpretation, this method, based on RE resolution, requires higher temporal resolution data and is, here, partly redundant with the WTF approach (analysis of the same signal). Hence, the model application requires specific conditions that restrict the number of events which can be interpreted, as compared with the WTF method. Among the major infiltration events presented in Table 2, only the hourly piezometric and weather records showing equivalent groundwater recession slopes before and after the piezometric rise were used. This constraint allows a clear detrending of the hydraulic head time variation to obtain the pure infiltration signal.

In addition, similarly to the WTF method, some rainfall events can also present small precipitated volumes, which do not cause a piezometric rise, i.e. unsaturated zone water retention (modified by evapotranspiration), producing some overestimation of the specific yield. Consequently, in view of the limited number of events which can be interpreted, the uncertainty cannot be reduced by multiple applications of the method as done for the WTF approach, except at P18B where two
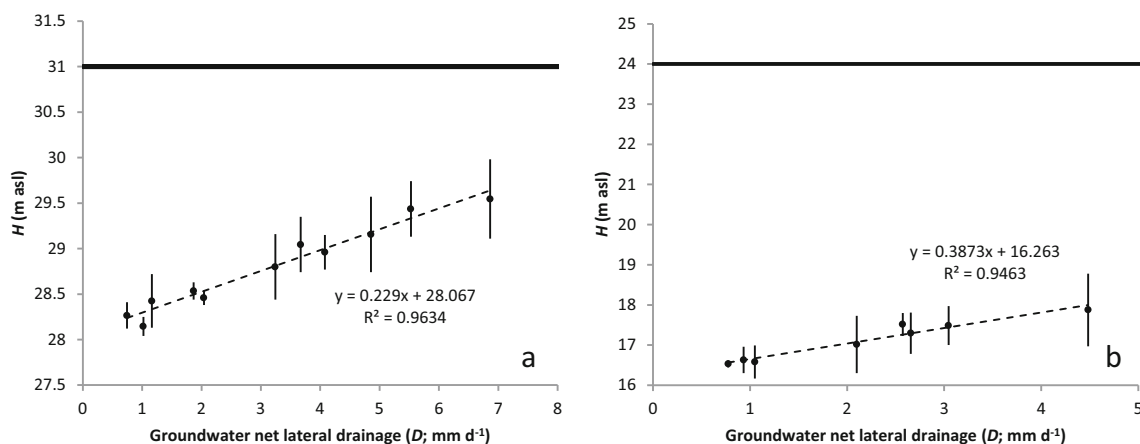

Fig. 4 Net groundwater drainage rate (*D*) as a function of the mean hydraulic head (*H*) of each WTF interpretation for piezometers **a** P42B and **b** P29B. Bold lines represent the topographic surface at each piezometer, and error bars represent the amplitude of the water-table fluctuations of each studied infiltration event

Table 4 Results obtained using the three different approaches to infer specific yields. SD stands for standard deviation

| Piezometers						Infiltration model		WTF method			Hydro-gravimetry		
BRGM code	ID	Network	X (WGS84)	Y (WGS84)	Meteorological station	S_y	SD	No. of events	S_y	SD	S_y using mean ΔS	S_y using NOAH ΔS	SD
09933X0088	88F	BRGM	4.93487	43.68011	Salon	–	–	2	7.9%	2.4%	1.1%	2.6%	2.3%
10192X0094	94F	BRGM	4.85507	43.4759	Istres	–	–	4	18.1%	3.3%	–	–	–
09934X0087	P18B	BRGM	4.9633	43.65283	Salon	10.8%	0.8%	3	11.5%	0.9%	18.1%	20.6%	3.9%
09937X0134	P19T	BRGM	4.92382	43.60907	Istres	–	–	5	5.0%	1.0%	17.6%	-4.0%	34.4%
10192X0095	P21B	BRGM	4.8114	43.5399	Istres	–	–	3	12.4%	0.5%	-5.8%	-13.2%	11.9%
09937X0135	P23B	BRGM	4.87195	43.57819	Istres	–	–	4	3.5%	0.6%	-15.5%	-126.4%	178.7%
10193X0151	P29B	BRGM	4.89617	43.55071	Istres	–	–	2	8.3%	0.5%	19.0%	8.3%	17.1%
09937X0133	P42B	BRGM	4.86231	43.60812	Istres	17.0%	–	2	9.2%	1.5%	-4.1%	4.1%	13.0%
09941X0261	PZ1	SYMCRAU	5.05259	43.6546	Salon	–	–	3	6.3%	0.6%	12.1%	15.7%	9.4%
10197X0554	PZ10	SYMCRAU	4.92877	43.45508	Istres	–	–	5	12.3%	1.5%	–	–	–
10193X0169	PZ11	SYMCRAU	4.90852	43.50369	Istres	–	–	2	12.3%	1.3%	51.1%	32.4%	29.9%
09936X0141	PZ13	SYMCRAU	4.82014	43.5786	Istres	–	–	4	8.5%	0.5%	–	–	–
09936X0138	PZ14	SYMCRAU	4.83842	43.63877	Istres	–	–	4	16.5%	2.2%	–	–	–
09936X0142	PZ15	SYMCRAU	4.78753	43.63581	Arles	–	–	5	10.4%	3.7%	26.3%	44.9%	29.6%
09945X0264	PZ16	SYMCRAU	5.05782	43.6305	Salon	–	–	4	7.5%	2.1%	6.9%	12.3%	14.2%
09935X0150	PZ17	SYMCRAU	4.73135	43.58632	Arles	–	–	3	4.0%	0.4%	–	–	–
09936X0143	PZ18	SYMCRAU	4.77286	43.57821	Arles	–	–	2	8.4%	0.6%	67.7%	8.1%	96.0%
10193X0170	PZ19	SYMCRAU	4.88875	43.52455	Istres	–	–	2	9.1%	1.1%	6.9%	3.0%	6.2%
09924X0136	PZ20	SYMCRAU	4.66202	43.66105	Arles	6.5%	–	3	3.6%	0.6%	-11.9%	-7.4%	5.1%
09931X0263	PZ21	SYMCRAU	4.72954	43.67315	Arles	–	–	2	2.9%	0.8%	5.7%	7.3%	1.8%
09934X0091	PZ22	SYMCRAU	5.01796	43.67818	Salon	–	–	3	12.7%	2.8%	-6.1%	14.6%	53.9%
09941X0262	PZ23	SYMCRAU	5.08277	43.67305	Salon	–	–	5	26.0%	6.2%	–	–	–
09935X0151	PZ24	SYMCRAU	4.68413	43.59025	Arles	7.5%	–	4	4.7%	1.1%	37.3%	74.3%	42.1%
09937X0156	PZ3	SYMCRAU	4.87098	43.63864	Istres	–	–	4	3.5%	0.7%	1.3%	10.4%	14.5%
09938X0184	PZ5	SYMCRAU	4.99765	43.63866	Salon	–	–	2	11.3%	0.6%	15.4%	16.8%	3.8%
09938X0189	PZ6	SYMCRAU	4.9803	43.60608	Salon	–	–	2	10.2%	1.9%	10.0%	13.1%	4.8%
10194X0257	PZ8	SYMCRAU	4.9666	43.53273	Istres	–	–	2	12.8%	0.7%	-1.3%	5.7%	11.1%
10194X0258	PZ9	SYMCRAU	4.96426	43.49161	Istres	–	–	6	5.6%	0.9%	31.0%	44.0%	20.8%
09938X0187	QUANT2	SYMCRAU	5.01988	43.64656	Salon	–	–	2	8.0%	0.6%	–	–	–
09937X0159	QUANT4	SYMCRAU	4.92471	43.64036	Istres	–	–	3	6.9%	0.4%	2.5%	8.1%	8.8%
10194X0259	QUANT7	SYMCRAU	4.96884	43.55813	Istres	9.0%	–	2	8.9%	0.2%	13.1%	19.4%	10.1%

Fig. 5 Parameter space 2D maps representing the RMSE function of the permeability Ks, the pore-size distribution index λ, and the specific yield Sy of the 22nd of October 2009 rainfall event at **a** piezometer P42B; **b** observed and simulated piezometry
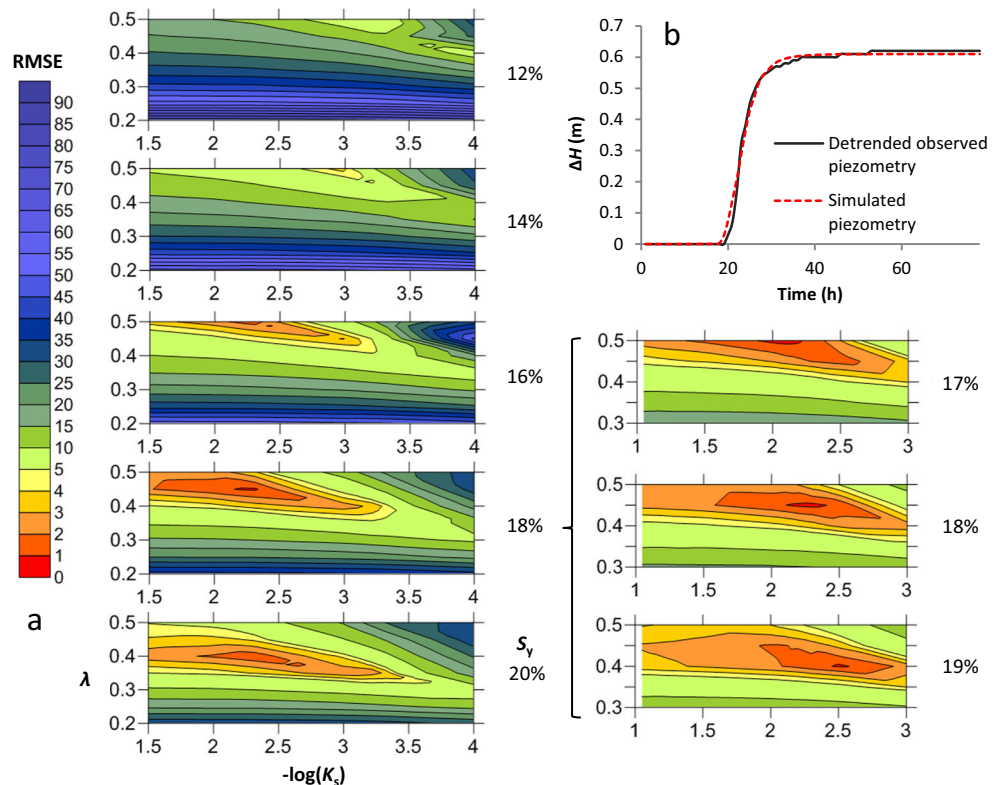
events were simulated (with $K_s = 10^{-3}$ m s^{-1} and $\lambda = 0.45$) leading to an average specific yield of $10.8 \pm 0.8\%$, consistent with the WTF result (Table 4).

Despite these limitations, the infiltration method can nevertheless be locally advocated for alluvial aquifers, especially in the absence of hydrodynamic parameters. Therefore, with

Fig. 6 Results of hydro-gravimetric surveys (September 2014 and March 2015) showing piezometric variations (ΔH) as a function of the gravimetric variations (Δg) represented by black dots. Red dots represent the piezometers that are excluded from the regression, gray dots represent data after NOAH soil moisture correction, and dashed lines are the linear regressions performed on raw and corrected data
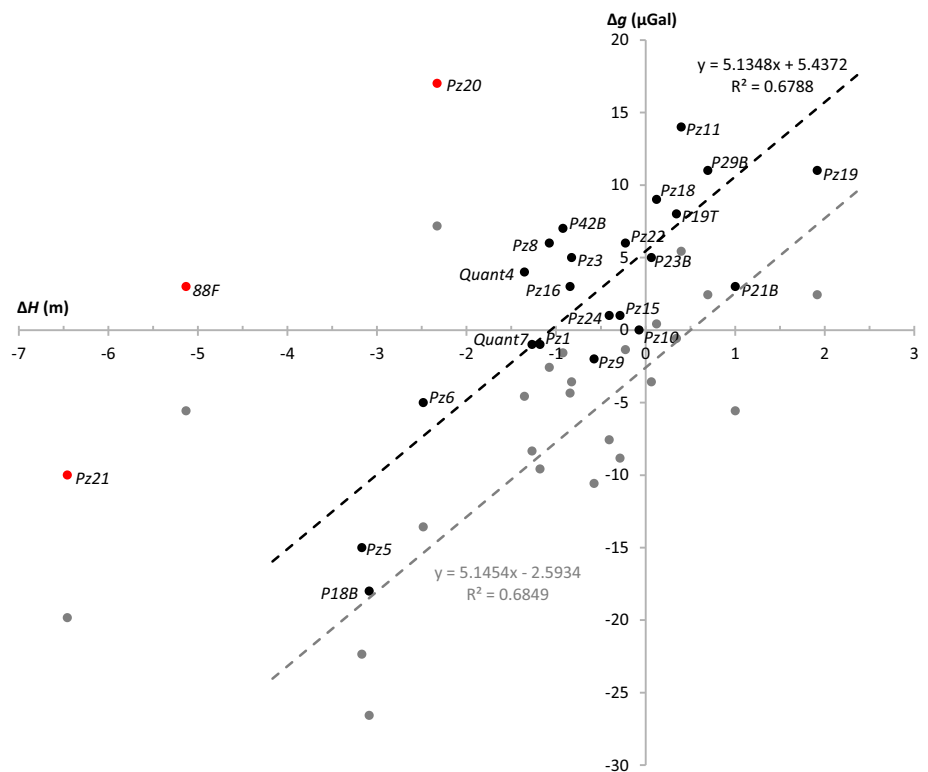
minimal data requirements, i.e. rainfall and water-table elevation at a unique piezometer, this approach can provide a first complete set of key parameters, i.e. hydraulic conductivity and specific yield.

Hydro-gravimetry

As previously mentioned, rainfall events occurring before and during the hydro-gravimetric surveys reduced the piezometric level variations between the two campaigns (i.e. increased the errors of calculated specific yields), and increased water storage effects within the unsaturated zone, which is difficult to ascertain. Hence, this technical limitation impacts the point-scale results of this hydro-gravimetric approach (see section 'Point-scale measurements'). Nevertheless, using the mean and NOAH soil moisture corrections (Fig. 6) improves the quality of the estimates provided by gravity variations due solely to water-table fluctuations, while preserving the same average regional specific yield (i.e., same regression slopes).

Comparison of the three methods

The infiltration model developed for this study to solve the RE involves costly time- and CPU-consuming simulations. In addition, the more difficult calibration process together with the specific conditions required (hourly piezometric and weather records, equal groundwater recession slopes before and after the piezometric rise) may limit the number of possible applications (see section 'One-dimensional infiltration model: discussion'). In the specific case of the Crau plain, this method is less efficient as compared to the very straightforward application of the WTF method.

The interpretation of the hydro-gravimetric surveys yields a $12.3 \pm 1.9\%$ mean regional specific yield for the entire aquifer, consistent with the value of 9.8% obtained by averaging the values provided by the WTF approach (Table 2), excluding the three points not accounted for in the hydro-gravimetric computation because of the local presence of clay beds (i.e. Pz20, Pz21, 88F; see section 'Average value of S_y at the aquifer scale'). The difference may be due to the different prospecting areas for each method. Gravity measurements present lateral resolutions that increase tenfold with the water-table depth (McCulloh 1965), leading to averages 49 and 60 m radius of lateral resolution for the high and low water periods, respectively (1st and 2nd campaigns). To quantify the lateral resolution of the S_y resulting from the two other methods (i.e. WTF approach and 1D infiltration model), it was proposed to apply the expression of the radius of action (R) of the water-table variation induced by uptake (Eq. 13, using

Dupuit's formula; De Marsily 1986) to estimate the radius of action of the rapid recharge event being studied:

$$R(t) = 1.5 \sqrt{\frac{T\,t}{S}} \tag{13}$$

Using an average $T = 3.10^{-2}$ m^2 s^{-1} (Seraphin 2016), the average $S_y = 0.98$ obtained with the WTF approach, and the mean duration of the studied events $t = 7.4\,10^5$ s (i.e. 8.7 days; Table 2), leads to an average radius of action $R = 231$ m, assuming that the uptake and infiltration processes involve the same physic. This suggests that the WTF approach and the 1D infiltration model would lead to specific yield estimates presenting lateral resolutions 3–4 times larger than the average one of the hydro-gravimetric method.

Figure 7a,b presents comparisons of specific yield values obtained using mean or NOAH gravimetric corrections, and the WTF method. Although the use of the NOAH data does not yield a perfect agreement (11 points with a 5% difference out of the 17 realistic specific yield values inferred from gravimetry; Fig. 7b), it provides a substantial improvement (assuming that the most reliable S_y estimates are obtained by the WTF method) as compared to the use of a mean soil moisture correction (9 points with a 5% difference out of the 16 realistic specific yield values inferred from gravimetry; Fig. 7a). This suggests that relevant estimates of the soil moisture variations with a better resolution (model and measurements) should be able to improve the local interpretations of the gravity field campaigns. Although relevant regional specific yield and unsaturated zone water storage variations were ascertained, this method would be more accurate for larger aquifers. Given the lack of efficiency of the other two methods and the independent validation of the WTF approach (see section 'Method validation'), this study considers the latter as the most reliable method to assess the spatial distribution of the specific yield for the Crau plain.

Specific yield spatial distribution and global groundwater budget

In the light of the comparison made in the previous section, the WTF results were used to describe the specific yield spatial distribution over the Crau aquifer. These 37 data were used in a geostatistical analysis with the "R" statistical software (Ihaka and Gentleman 1996). The interpolation of the logarithm of the specific yield data by kriging on a regular grid spacing (100 × 100 m) was performed by fitting a spherical model (sill = 0.05, range = 10,000 m, nugget = 0) to the empirical variogram (sample variance = 0.051; Fig. 8), leading to a spatial distribution of the specific yield (Fig. 8) with a satisfying resolution and a 9.1% regional mean value (weighted by water content of each mesh). This new spatial distribution suggests an expected correlation between the specific yield and the geology. Most of

Fig. 7 Comparison of specific yields computed by the WTF method as a function of their counterpart from the hydro-gravimetry method using **a** average soil moisture data and **b** NOAH soil moisture data. Dashed lines represent a 5% interval error (because of their irrelevance, standard deviations of the gravimetric method are not represented)
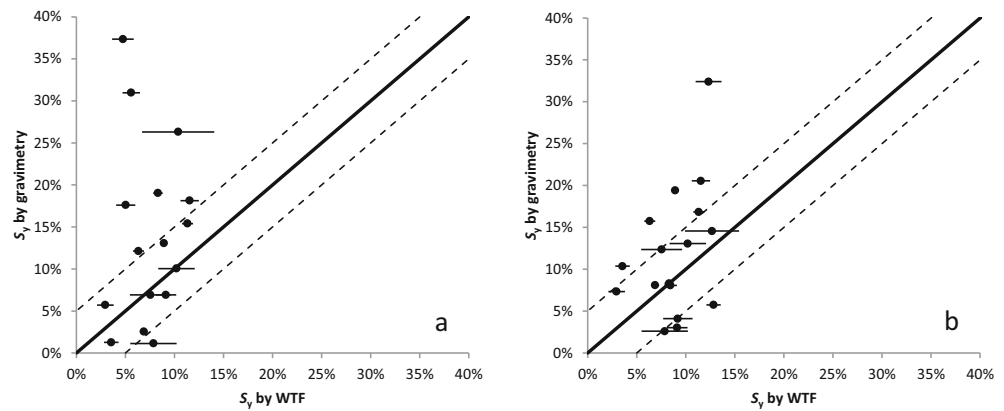
the values above 10% are located where the alluvial deposits are thick (above 20 m), and probably less cemented. Clay banks have been observed at the two piezometers (Pz20 and Pz21) in the north-west part of the Crau plain, explaining the low specific yield in this part of Fig. 8.

The relevance of the specific yield spatial distribution obtained in this study can be verified using the global groundwater mass balance of the Crau aquifer which is written during a given time period:

$$\iiint_{h_i}^{h_f} S_y(x,y)\, dh\, dx\, dy = \int_{t_i}^{t_f} (R_i + R_n + Q_{in} - Q_{out} - U)\, dt \quad (14)$$

and involves all the groundwater fluxes circulating in the aquifer: the recharge by irrigation return flow (R_i), the natural

recharge (R_n), the upstream and downstream groundwater lateral flows (Q_{in} and Q_{out}), and the overall uptakes (U). The mass balance Eq. (14) is written, for an average year, over the period from 15 March (t_i in Eq. 14) to 15 October (t_f), corresponding to the irrigation period in order to maximize the specific yield effect (maximal water-table fluctuations). The right-hand side of Eq. (14) can be computed using the fluxes independently obtained using a stable isotope-mixing model (Seraphin et al. 2016). According to this study, for the 7-month time period considered here, the recharge by irrigation return flow (R_i) and the natural recharge (R_n) were 4.92 ± 0.89 and 1.17 ± 0.50 m^3 s^{-1}, respectively. Note that, assuming a constant infiltration process, R_n was weighted using the average proportion of precipitation during this time period
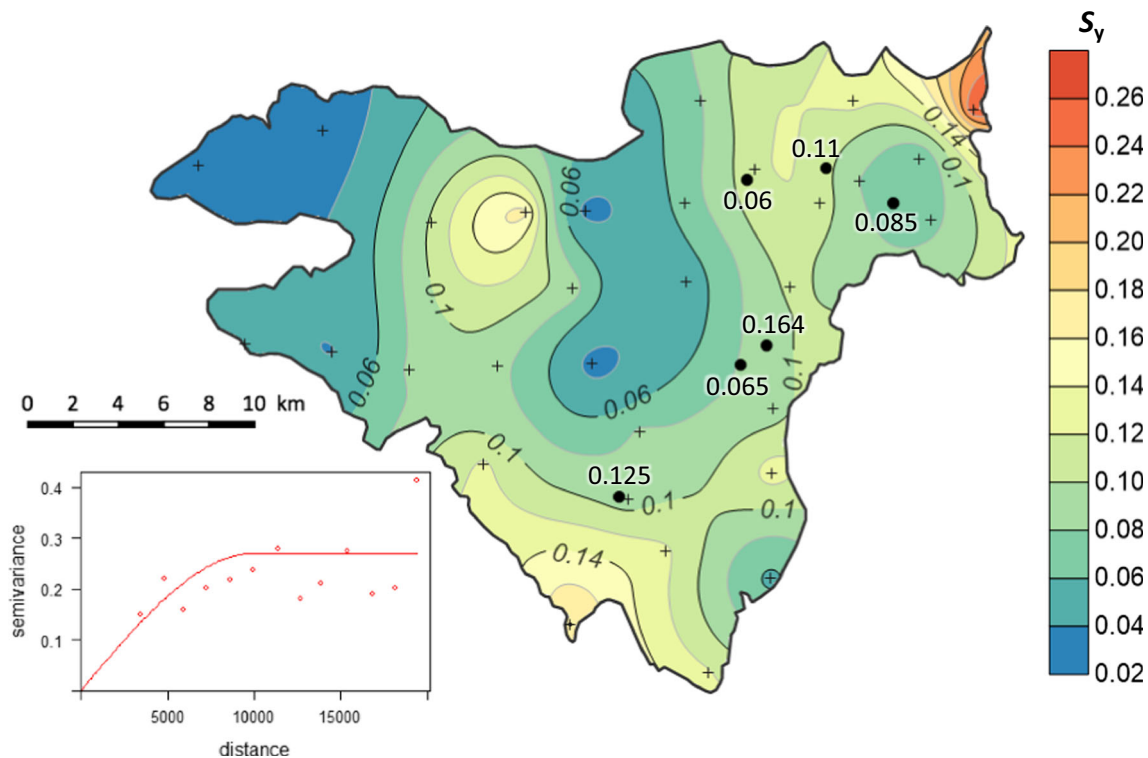

Fig. 8 Spatial distribution of the specific yield, obtained by interpolating (kriging) the results of the WTF method, and its associated variogram. Black dots represent the specific yield estimates of previous studies, and black crosses represent the location of the points used for the interpolation

(53.4% of the annual mean rainfall, computed with 1991–2015 meteorological data). The uptakes (U) represent 1.52 ± 0.24 m^3 s^{-1}, the upstream groundwater lateral inflow (Q_{in}), 0.48 m^3 s^{-1}, and the natural discharge (Q_{out}), 3.12 ± 0.20 m^3 s^{-1}. Using these previous independent estimates, the right-hand side of the groundwater budget described in Eq. (14) yields a value of $3.57 \pm 0.98 \times 10^7$ m^3 for the groundwater storage variation in the aquifer between March 15th and October 15th. The left-hand side of Eq. (14) now can be computed using the specific yield spatial distribution obtained here to verify the consistency with the above calculation. Similar to the specific yield, the average water-table variations of 31 piezometers over this period (average variations computed between March 15th and October 15th for years 2013 and 2014, the period optimizing the number of piezometers with daily records) were interpolated by kriging. Then, the sum of the specific yield times the water-table variation for each mesh yields the required net overall groundwater storage variation in the aquifer between 15 March and 15 October (left-hand side of Eq. 14). The value obtained by this calculation, 3.09×10^7 m^3, is in excellent agreement with the aforementioned independent estimate ($3.57 \pm 0.98 \times 10^7$ m^3) and reinforces the relevance of this study.

Conclusions

Observed in monitored boreholes, multiple large infiltration processes caused by large precipitation events were interpreted in terms of specific yield by means of the WTF method and a 1D vertical numerical model solving the RE in the unsaturated zone. Both of these methods are sensitive to the assumption of recharge by the entire rainfall volumes and the heterogeneity of the precipitation events, but the WTF interpretation of multiple major events for each piezometer yields relevant results and reduces the impact of these limitations. Assuming that the most reliable S_y estimates are obtained by the WTF method, and despite the low signal, the gravimetric method provides a valuable regional specific yield consistent with the results of the WTF method. The local bias of the hydro-gravimetric method, due to soil water storage, can be partially eliminated using widely available NOAH soil moisture data, but does not lead to relevant local specific yields in this case. Since this method is redundant for S_y with the WTF approach, the infiltration method, which is more time-consuming, should be limited to areas where additional hydraulic conductivity values are desirable (unsampled areas). The range of local specific yields obtained by the WTF method (2.9–26%) is in line with the scarce data available so far. Hence, the first regionalized map of the specific yield of this aquifer of major economic importance is proposed here, making it possible to build an accurate transient model based on parameter values independent from any prior hydrogeological

modeling. Tested by means of a simple mass balance calculation over the Crau plain, the estimates obtained here are consistent with the overall groundwater budget recently calculated using stable isotopes, showing the robustness of these methods. Additional parameters can be obtained by the alternative approaches proposed here: the infiltration model provides permeability, the WTF method offers the opportunity to independently estimate mean recharges (using the relationship between net groundwater drainage and hydraulic head; see section 'Method validation'), and hydro-gravimetry can estimate an average soil moisture variation. In a context of climate change implying more frequent extreme rainfall events, the authors believe that these approaches would produce more accurate and relevant results for other large unconfined aquifers, compared to the commonly performed spatial calibration of the specific yield through hydrogeological modeling.

References

Albinet M, Bonnet M, Colomb E, Cornet G (1969) Carte hydrogéologique de la France, 993-1019, Istres-Eyguières, Plaine de la Crau [Hydrogeological map of France, 993-1019, Istres-Eyguières, Crau plain]. 1/50000. BRGM, Orleans, France

ANTEA (1995) Municipality of Salon de Provence (13) - Application for authorization to use water taken from the natural environment [Commune de Salon de Provence (13) - Demande d'autorisation d'utilisation d'eau prélevée dans le milieu naturel].

Bader J-C, Saos J-L, Charron F (2010) Modèle de ruissellement, avancement et infiltration pour l'irrigation à la planche Sur un sol recouvrant un sous-sol très perméable [Runoff, advancement and infiltration model for board irrigation method on a soil covering a highly permeable subsoil]. Hydrol Sci J 55:177–191. https://doi.org/10.1080/02626660903546050

Becker M, Meyssignac B, Xavier L, Cazenave A, Alkama R, Decharme B (2011) Past terrestrial water storage (1980–2008) in the Amazon Basin reconstructed from GRACE and in situ river gauging data. Hydrol Earth Syst Sci 15:533–546. https://doi.org/10.5194/hess-15-533-2011

Beilin J (2006) Apport de la gravimétrie absolue à la réalisation de la composante gravimétrique du Réseau Géodésique Français [Contribution of absolute gravimetry to the realization of the gravimetric component of the French Geodetic Network]. Inst. Géographique National, Saint-Mandé, France

Berard P, Daum JR, Martin JC (1995) "MARTCRAU": actualisation du modèle de la nappe de la Crau ["MARTCRAU": updating the Crau aquifer model]. BRGM, Orleans, France

Beven K (1993) Prophecy, reality and uncertainty in distributed hydrological modelling. Adv Water Resour 16:41–51

Boissard G (2009) Geological and hydrogeological synthesis. Quantitative assessment of the impact on the water resource [Synthèse géologique et hydrogéologique. Évaluation quantitative de l'impact sur la ressource en eau], Report F, ICF Environnement.

Bonnet M, Clouet D'Orval M, Friedlaender M, Margat J (1972) Etude de l'infiltration dans les nappes libres: essai d'identification automatique par modèles inverses—application à la nappe de la Crau [Study of infiltration in unconfined aquifers: automated identification by inverse models—application to the Crau aquifer]. BRGM, Orleans, France

Bonvalot S, Remy D, Deplus C, Diament M, Gabalda G (2008) Insights on the March 1998 eruption at Piton de la Fournaise volcano (La Reunion) from microgravity monitoring. J Geophys Res Solid Earth 113(B5):B05407

BRGM (2016a) Portail national d'accès aux données sur les eaux souterraines (ADES) [National portal for access to groundwater data (ADES)]. BRGM, Orleans, France. http://www.ades.eaufrance.fr/. Accessed March 2018

BRGM (2016b) Banque de données du Sous-Sol (BSS) [Underground database (BSS)]. BRGM, Orleans, France. http://infoterre.brgm.fr/. Accessed March 2018

Brooks RH, Corey AT (1964) Hydraulic properties of porous media and their relation to drainage design. Trans ASAE 7:26–28

Chapman DS, Sahm E, Gettings P (2008) Monitoring aquifer recharge using repeated high-precision gravity measurements: a pilot study in South Weber, Utah. Geophysics 73:WA83–WA93

Christiansen L, Binning PJ, Rosbjerg D, Andersen OB, Bauer-Gottwein P (2011) Using time-lapse gravity for groundwater model calibration: an application to alluvial aquifer storage. Water Resour Res 47:12. https://doi.org/10.1029/2010WR009859

Colomb E, Roux MR (1978) La Crau, données nouvelles et interprétations [The Crau plain, new data and interpretations]. Géol Mediterr 5:303–324

Courault D, Hadria R, Ruget F, Olioso A, Duchemin B, Hagolle O, Dedieu G (2010) Combined use of FORMOSAT-2 images with a crop model for biomass and water monitoring of permanent grassland in Mediterranean region. Hydrol Earth Syst Sci 14:1731–1744. https://doi.org/10.5194/hess-14-1731-2010

Crosbie RS, Binning P, Kalma JD (2005) A time series approach to inferring groundwater recharge using the water table fluctuation method. Water Resour Res 41:9. https://doi.org/10.1029/2004WR003077

Cuthbert MO (2010) An improved time series approach for estimating groundwater recharge from groundwater level fluctuations. Water Resour Res 46:11. https://doi.org/10.1029/2009WR008572

Cuthbert MO (2014) Straight thinking about groundwater recession. Water Resour Res 50:2407–2424. https://doi.org/10.1002/2013WR014060

De Marsily G (1986) Quantitative hydrogeology. Paris School of Mines, Fontainebleau, France

Dean JF, Webb JA, Jacobsen GE, Chisari R, Dresel PE (2015) A groundwater recharge perspective on locating tree plantations within low-rainfall catchments to limit water resource losses. Hydrol Earth Syst Sci 19:1107–1123. https://doi.org/10.5194/hess-19-1107-2015

Dellery B, Durozoy G, Forkasiewicz J, Gouvernet C, Margat J (1964) Etude hydrogéologique de la Crau [Hydrogeological study of the Crau plain]. BRGM, Orleans, France

Deville S (2013) Caractérisation de la zone non saturée des karsts par la gravimétrie et l'hydrogéologie [Characterization of the unsaturated zone of karsts by gravimetry and hydrogeology]. Université Montpellier II-Sciences et Techniques du Languedoc, Montpellier, France

Fiedler FR (2003) Simple, practical method for determining station weights using Thiessen polygons and isohyetal maps. J Hydrol Eng 8:219–221

Forkasiewicz J (1972) Practical workbook of pumping tests interpretation [Cahier des travaux pratiques d'interprétation des pompages d'essai], BRGM.

Garnier JL, Syssau A (1976) Final report of hydrogeological monitoring of the drilling of the société Lorraine-Provence in Saint Martin de Crau (Bouches du Rhône) [Rapport final de surveillance hydrogéologique du forage de la société Lorraine-Provence à Saint Martin de Crau (Bouches du Rhône)], BRGM.

GO-13 (2009) MNT 2009 5 m - DEPT 13 (DTM 2009 5 m - DEPT 13). CRIGE-PACA, Aix-en-Provence, France. http://www.crige-paca.org/. Accessed March 2018

Gonçalvès J, Petersen J, Deschamps P, Hamelin B, Baba-Sy O (2013) Quantifying the modern recharge of the "fossil" Sahara aquifers. Geophys Res Lett 40:2673–2678

Hall DW, Risser DW (1993) Effects of agricultural nutrient management on nitrogen fate and transport in Lancaster County Pennsylvania. J Am Water Resour Assoc 29:55–76. https://doi.org/10.1111/j.1752-1688.1993.tb01504.x

Healy RW, Cook PG (2002) Using groundwater levels to estimate recharge. Hydrogeol J 10:91–109. https://doi.org/10.1007/s10040-001-0178-0

Hector B, Seguis L, Hinderer J, Descloitres M, Vouillamoz JM, Wubda M, Boy JP, Luck B, Le Moigne N (2013) Gravity effect of water storage changes in a weathered hard-rock aquifer in West Africa: results from joint absolute gravity, hydrological monitoring and geophysical prospection. Geophys J Int 194:737–750. https://doi.org/10.1093/gji/ggt146

Heliotis FD, DeWitt CB (1987) Rapid water table responses to rainfall in a northern peatland ecosystem. J Am Water Resour Assoc 23:1011–1016. https://doi.org/10.1111/j.1752-1688.1987.tb00850.x

Howle JF, Phillips SP, Denlinger RP, Metzger LF (2003) Determination of specific yield and water-table changes using temporal microgravity surveys collected during the second injection, storage, and recovery test at Lancaster, Antelope Valley, California, November 1996 through April 1997. US Geological Survey, Reston, VA

Hwang C, Wang C-G, Lee L-H (2002) Adjustment of relative gravity measurements using weighted and datum-free constraints. Computers Geosci 28:1005–1015. https://doi.org/10.1016/S0098-3004(02)00005-5

Ihaka R, Gentleman R (1996) R: a language for data analysis and graphics. J Comput Graph Stat 5:299–314

Jacob T (2009) Apport de la gravimétrie et de l'inclinométrie à l'hydrologie karstique [Contribution of gravimetry and inclinometry to karst hydrology]. PhD Thesis, Montpellier 2 University, Montpellier, France

Jacob T, Bayer R, Chery J, Jourde H, Le Moigne N, Boy JP, Hinderer J, Luck B, Brunet P (2008) Absolute gravity monitoring of water storage variation in a karst aquifer on the Larzac plateau (southern France). J Hydrol 359:105–117

Jacob T, Bayer R, Chery J, Le Moigne N (2010) Time-lapse microgravity surveys reveal water storage heterogeneity of a karst aquifer. J Geophys Res Solid Earth 115(6):B06402

Jie Z, van Heyden J, Bendel D, Barthel R (2011) Combination of soil-water balance models and water-table fluctuation methods for evaluation and improvement of groundwater recharge calculations. Hydrogeol J 19:1487–1502

Jourde H, Brunet P (2001) Report on the tracing test carried out on the SNCF railway station in Miramas (13) [Rapport relatif à l'essai de traçage réalisé sur la gare de triage SNCF de Miramas (13)]

Kroner C, Jahr T (2006) Hydrological experiments around the superconducting gravimeter at Moxa observatory. J Geodyn 41:268–275

Lederer M (2009) Accuracy of the relative gravity measurement. Acta Geodyn Geomater 6:155

Maier J (2010) Feasibility study for the management of groundwater pollution by the ANS - Assessment of the natural attenuation potential. 1: Hydrochemical and microbiological investigations [Etude de faisabilité pour la gestion de la pollution des eaux souterraines par l'ANS - Evaluation du potentiel d'atténuation naturelle. 1 : Investigations hydrochimiques et microbiologiques]. Report, ICF Environnement.

Mailhol JC, Merot A (2007) SPFC: a tool to improve water management and hay production in the Crau region. Irrig Sci 26:289–302. https://doi.org/10.1007/s00271-007-0099-3

Maréchal JC, Dewandel B, Ahmed S, Galeazzi L, Zaidi FK (2006) Combined estimation of specific yield and natural recharge in a semi-arid groundwater basin with irrigated agriculture. J Hydrol 329:281–293. https://doi.org/10.1016/j.jhydrol.2006.02.022

McCulloh TH (1965) A confirmation by gravity measurements of an underground density profile based on core densities. Geophysics 30:1108–1132

Melchior P (2008) Gravimetric measuring techniques. Phys Methods Instrum Meas Encycl Life Support Syst EOLSS 2:259–290

Merlet S, Kopaev A, Diament M, Geneves G, Landragin A, Dos Santos FP (2008) Micro-gravity investigations for the LNE watt balance project. Metrologia 45:265

Météo-France (2016) Données publiques climatiques [Public climate data]. https://donneespubliques.meteofrance.fr/. Accessed March 2018

Miller EE, Miller RD (1956) Physical theory for capillary flow phenomena. J Appl Phys 27:324–332. https://doi.org/10.1063/1.1722370

Millman KJ, Aivazis M (2011) Python for scientists and engineers. Comput Sci Eng 13:9–12. https://doi.org/10.1109/MCSE.2011.36

Montgomery EL (1971) Determination of coefficient of storage by use of gravity measurements. PhD Thesis, University of Arizona, Tucson, AZ

Moon S-K, Woo NC, Lee KS (2004) Statistical analysis of hydrographs and water-table fluctuation to estimate groundwater recharge. J Hydrol 292:198–209

NASA (2016) GLDAS data. In: Goddard Earth Sci. Data Inf. Serv. Cent. GES DISC. https://disc.sci.gsfc.nasa.gov/uui/datasets?keywords=GLDAS. Accessed March 2018

Naujoks M, Kroner C, Weise A, Jahr T, Krause P, Eisner S (2010) Evaluating local hydrological modelling by temporal gravity observations and a gravimetric three-dimensional model. Geophys J Int 182:233–249

Olioso A, Lecerf R, Baillieux A, Chanzy A, Ruget F, Banton O, Lecharpentier P, Trolard F, Cognard-Plancq AL (2013) Modelling of drainage and hay production over the Crau aquifer for analysing impact of global change on aquifer recharge. Procedia Environ Sci 19:691–700. https://doi.org/10.1016/j.proenv.2013.06.078

Oliphant TE (2007) Python for scientific computing. Comput Sci Eng 9:10–20. https://doi.org/10.1109/MCSE.2007.58

Park E, Parker JC (2008) A simple model for water table fluctuations in response to precipitation. J Hydrol 356:344–349

Pool DR, Eychaner JH (1995) Measurements of aquifer-storage change and specific yield using gravity surveys. Ground Water 33:425–432

Porchet M (1930) Etude des eaux souterraines de la Crau [Groundwater study of the Crau plain]. Ann Ministère Agric:203–223

Ramillien G, Frappart F, Seoane L (2014) Application of the regional water mass variations from GRACE satellite gravimetry to large-scale water management in Africa. Remote Sens 6:7379–7405. https://doi.org/10.3390/rs6087379

Rawls WJ, Brakensiek DL, Saxtonn KE (1982) Estimation of soil water properties. Trans ASAE 25:1316–1320

Rivière A, Gonçalvès J, Jost A, Font M (2014) Experimental and numerical assessment of transient stream–aquifer exchange during disconnection. J Hydrol 517:574–583. https://doi.org/10.1016/j.jhydrol.2014.05.040

Rodell M, Beaudoing HK (2013) NASA/GSFC/HSL (2013), GLDAS Noah Land Surface Model L4 monthly 0.25 × 0.25 degree Version 2.0, version 020, Greenbelt, Maryland, USA. Goddard Earth Sciences Data and Information Services Center (GES DISC), Greenbelt, MD

Scintrex Ltd. (2006) CG-5 Scintrex Autograv system operation manual. Scintrex, Concord, ON

Seraphin P (2016) Contribution du traçage isotopique (δ^{18}O et δD) à la compréhension et à la modélisation hydrogéologique de la nappe de la Crau [Contribution of isotopic tracing (δ^{18}O and δD) for understanding and hydrogeological modeling of the groundwater of the Crau aquifer]. PhD Thesis, Aix-Marseille Université, Marseille, France. https://doi.org/10.13140/RG.2.2.31645.41444

Seraphin P, Vallet-Coulomb C, Gonçalvès J (2016) Partitioning groundwater recharge between rainfall infiltration and irrigation return flow using stable isotopes: the Crau aquifer, France. J Hydrol. https://doi.org/10.1016/j.jhydrol.2016.09.005

Simunek J, Sejna M, Van Genuchten MT (1998) The Hydrus-1D software package for simulating the one-dimensional movement of water, heat, and multiple solutes in variably-saturated media. Version 2.0, IGWMC - TPS - 70, International Ground Water Modeling Center, Colorado School of Mines, Littleton, CO

Sophocleous MA (1991) Combining the soilwater balance and water-level fluctuation methods to estimate natural groundwater recharge: practical aspects. J Hydrol 124:229–241. https://doi.org/10.1016/0022-1694(91)90016-B

Vallet-Coulomb C, Seraphin P, Gonçalvès J, Radakovitch O, Cognard-Plancq AL, Crespy A, Babic M, Charron F (2017) Multi-approach quantification of groundwater recharge in the Crau Plain, France. J Hydrol. https://doi.org/10.1016/j.apgeochem.2017.10.001

Vereecken H, Kasteel R, Vanderborght J, Harter T (2007) Upscaling hydraulic properties and soil water flow processes in heterogeneous soils. Vadose Zone J 6:1–28. https://doi.org/10.2136/vzj2006.0055

Vogel T, Huang K, Zhang R, Van Genuchten MT (1996) The HYDRUS code for simulating one-dimensional water flow, solute transport, and heat movement in variably-saturated media. US Salinity Lab, Riverside, CA

Warrick AW, Hussen AA (1993) Scaling of Richards' equation for infiltration and drainage. Soil Sci Soc Am J 57:15. https://doi.org/10.2136/sssaj1993.03615995005700010004x

Weeks EP (2002) The Lisse effect revisited. Ground Water 40:652–656. https://doi.org/10.1111/j.1745-6584.2002.tb02552.x